

Design and Synthesis of Novel Anthracene Derivatives as n-type Emitters for Electroluminescent Devices: A Combined Experimental and DFT Study

G. Mallesham,^{a,b} S. Balaiah,^b M. Ananth Reddy,^{a,b} B. Sridhar,^{*c} Punita Singh,^d Ritu Srivastava,^{*d} K. Bhanuprakash^{*b,e} and V. Jayathirtha Rao^{*a,e}

^a Crop Protection Chemicals Division, ^b Inorganic and Physical Chemistry Division,

^c Laboratory of X-Ray Crystallography, Indian Institute of Chemical Technology, Hyderabad 500007, India

^d Organic Electronics, National Physical Laboratory, New Delhi, India

^e National Institute for Solar Energy, New Delhi, India

Supplementary information

Content

HOMO, LUMO energy levels calculated with B3LYP/6-311G(d,p).....	ii
ORTEP diagrams for 4b and 8c	iii
DSC thermo grams	iv
TGA plots.....	v-vii
UV-Vis and PL spectra in different solvents	viii-xiii
OLED device graphs	xiv-xix
Crystal data and structure refinement details for 4b and 8c	xx
UV-Vis absorption data (λ_{abs}) of 4a–4c and 8a–8c in different solvents	xxi
^1H and ^{13}C NMR spectra for 4a–4c and 8a–8c	xxii-xxvii

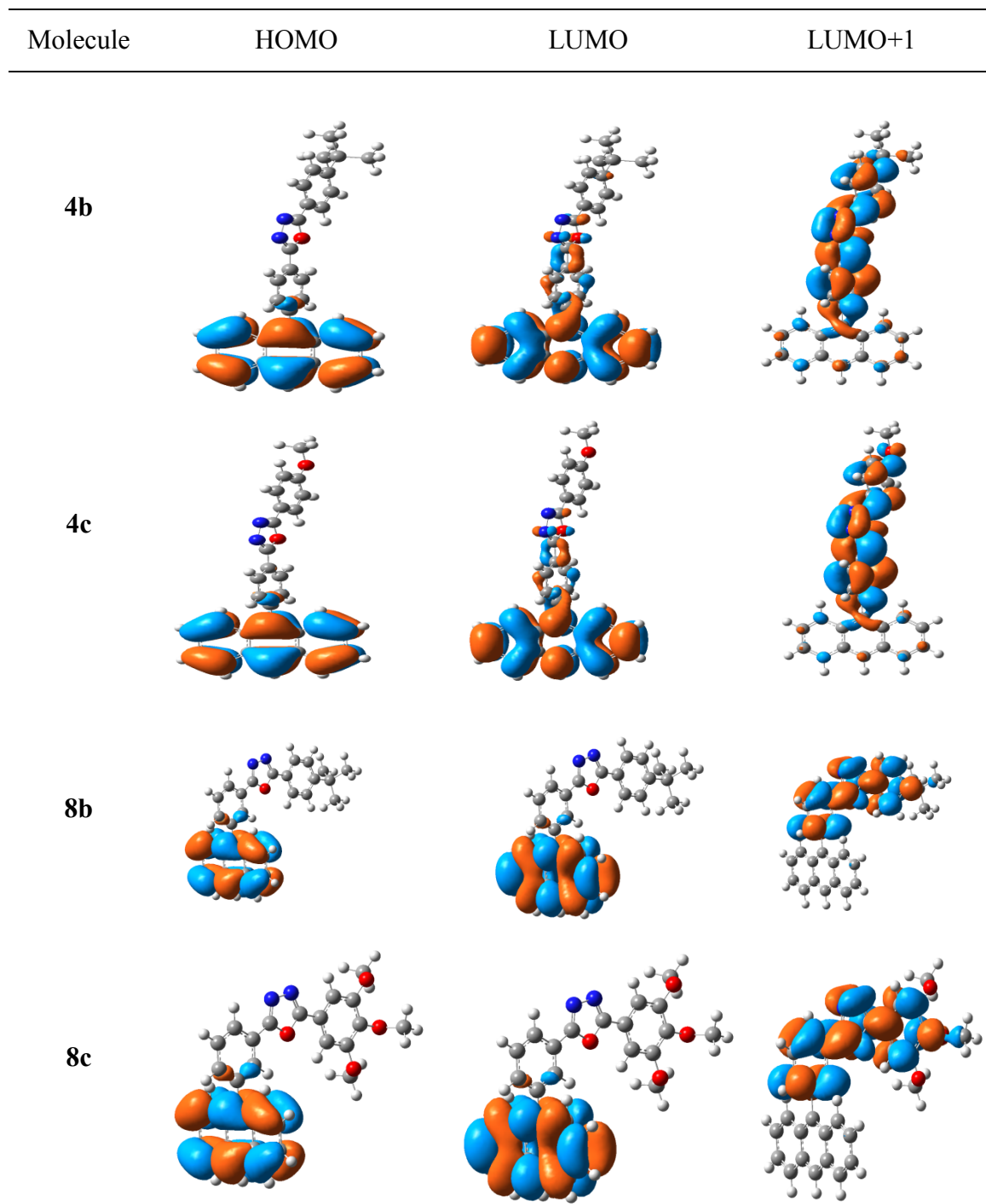
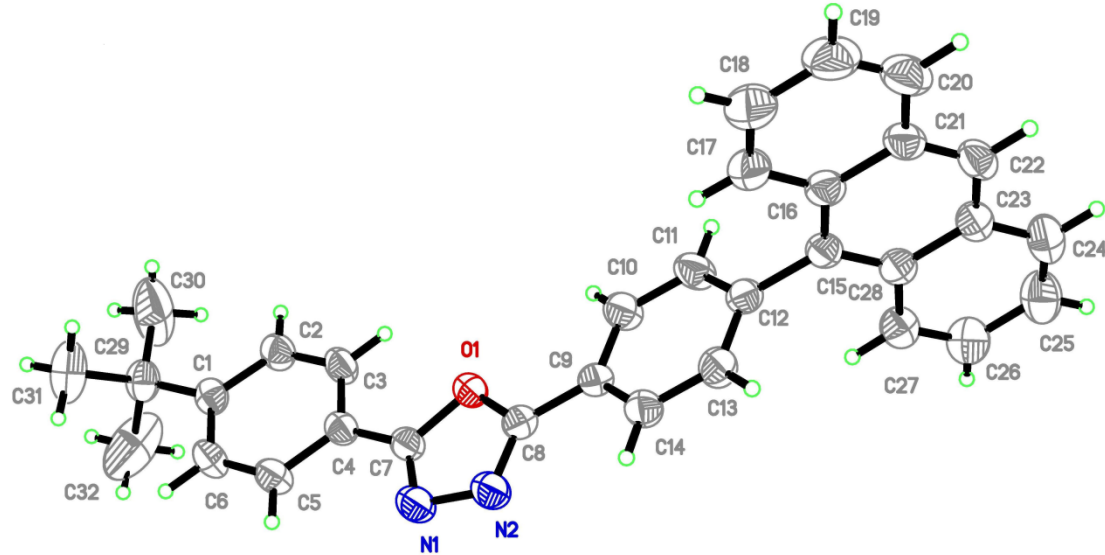


Fig. 1 Frontier molecular orbitals of **4b**, **4c**, **8b** and **8c** obtained at B3LYP/6-311G(d,p) level of theory

a)



b)

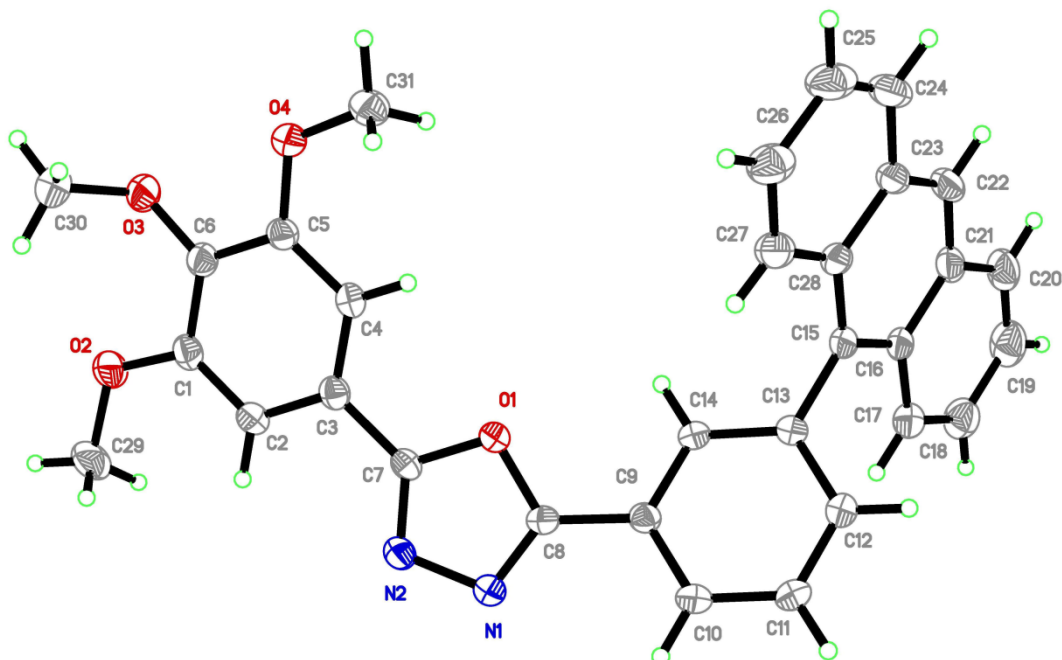


Fig. 2 ORTEP diagrams of 4b (a) and 8c (b).

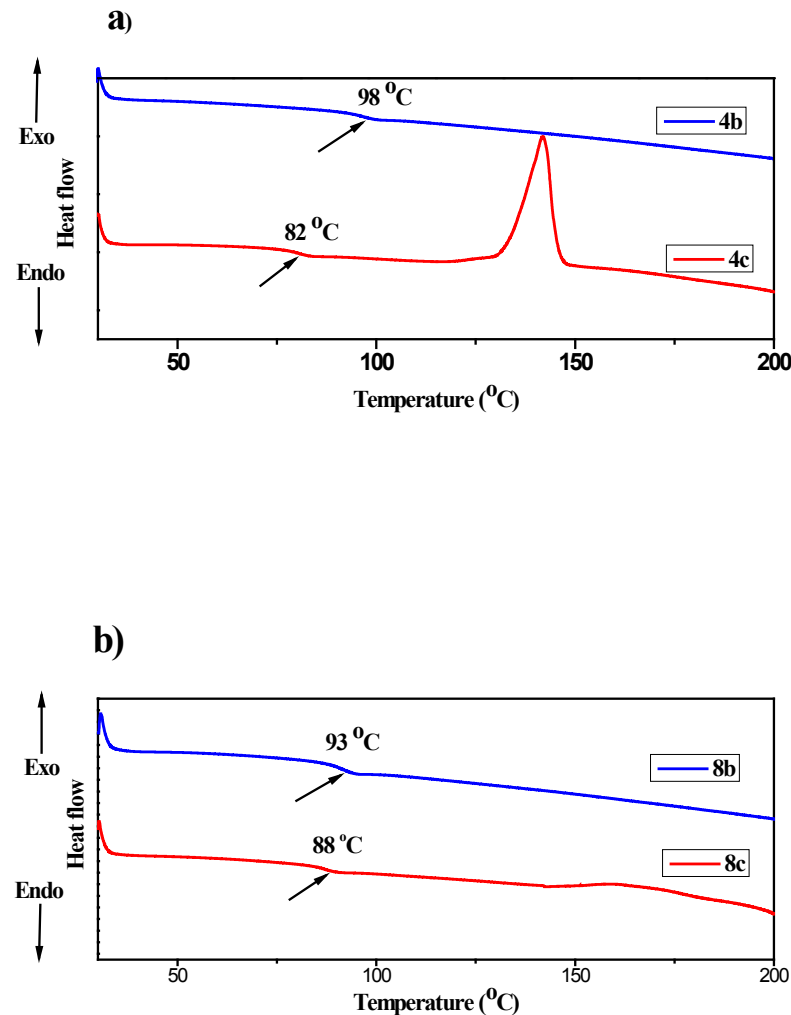


Fig. 3 DSC traces of 4b-4c (a) and 8b-8c (b).

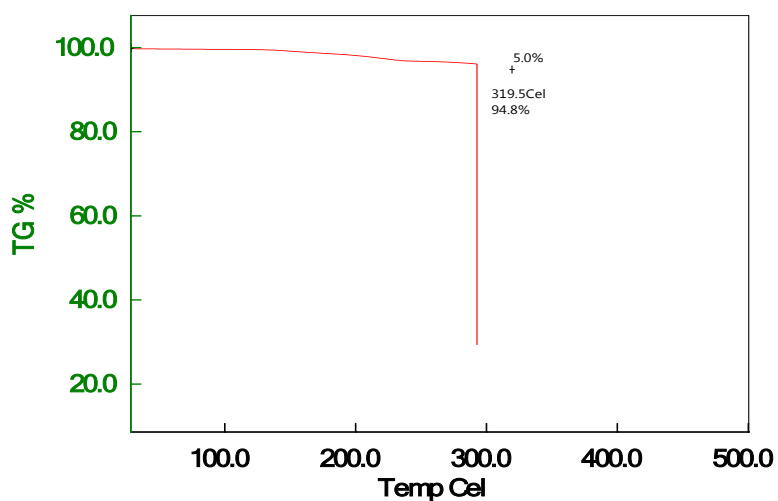


Fig. 4 TGA thermogram of **4a** recorded at a heating rate of $10\text{ }^{\circ}\text{C min}^{-1}$.

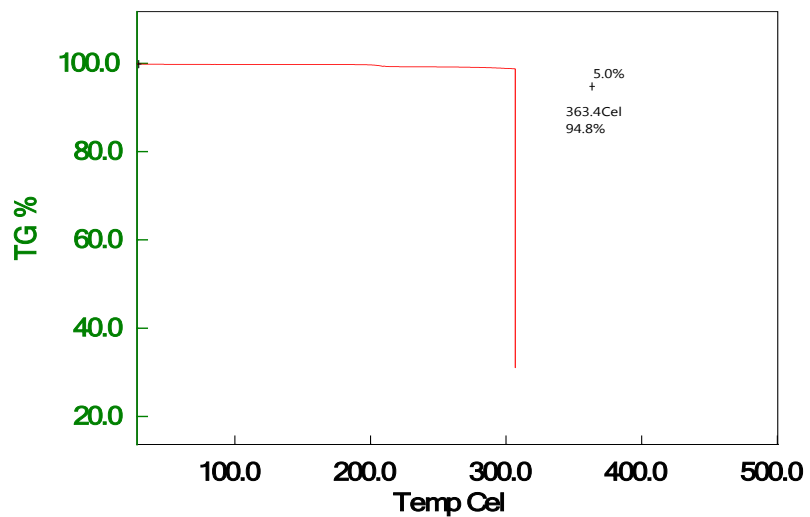


Fig. 5 TGA thermogram of **4b** recorded at a heating rate of $10\text{ }^{\circ}\text{C min}^{-1}$.

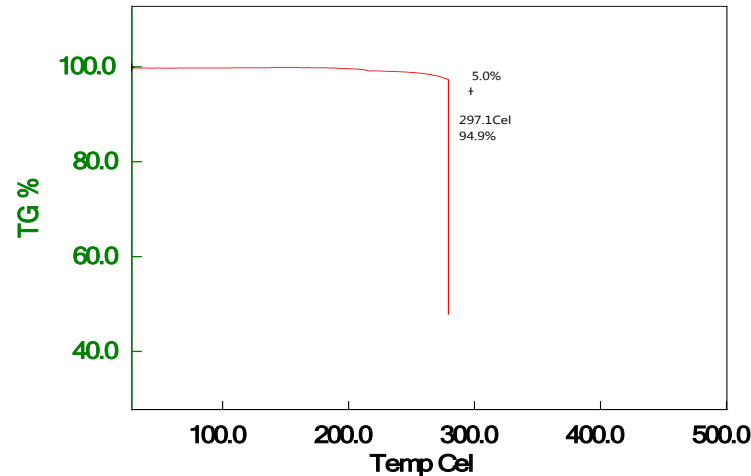


Fig. 6 TGA thermogram of **4c** recorded at a heating rate of $10\text{ }^{\circ}\text{C min}^{-1}$.

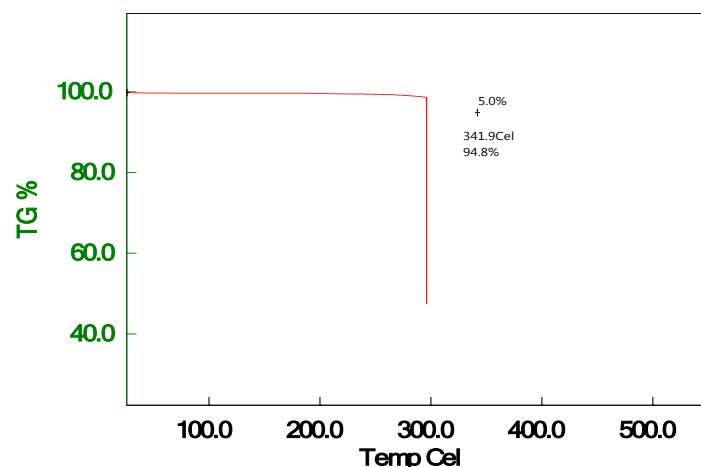


Fig. 7 TGA thermogram of **8a** recorded at a heating rate of $10\text{ }^{\circ}\text{C min}^{-1}$.

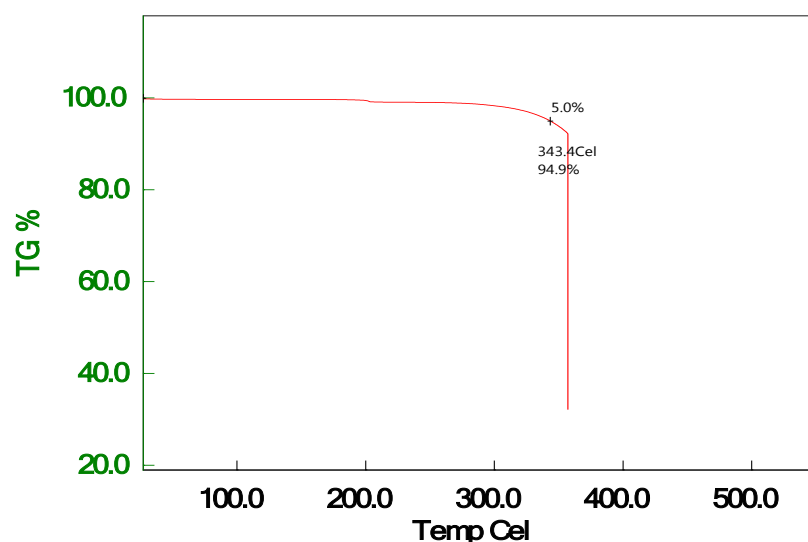


Fig. 8 TGA thermogram of **8b** recorded at a heating rate of $10\text{ }^{\circ}\text{C min}^{-1}$.

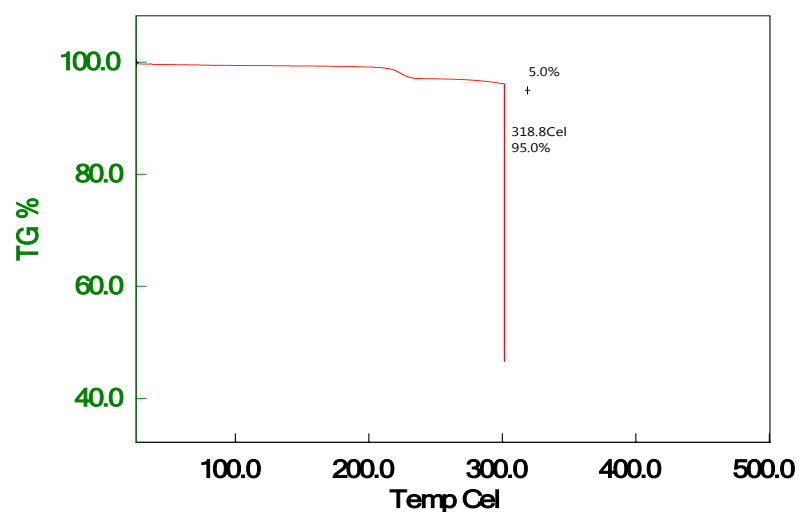


Fig. 9 TGA thermogram of **8c** recorded at a heating rate of $10\text{ }^{\circ}\text{C min}^{-1}$.

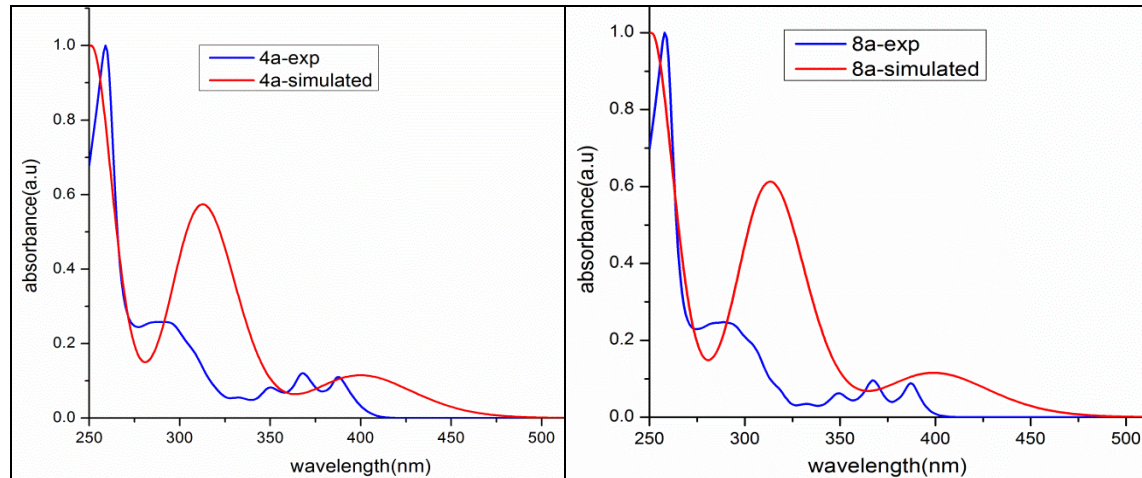


Fig 10: UV-Vis absorption spectra of compounds **4a** and **8a** obtained from experiment and B3LYP/6-311G(d,p) level in CHCl_3 solvent.

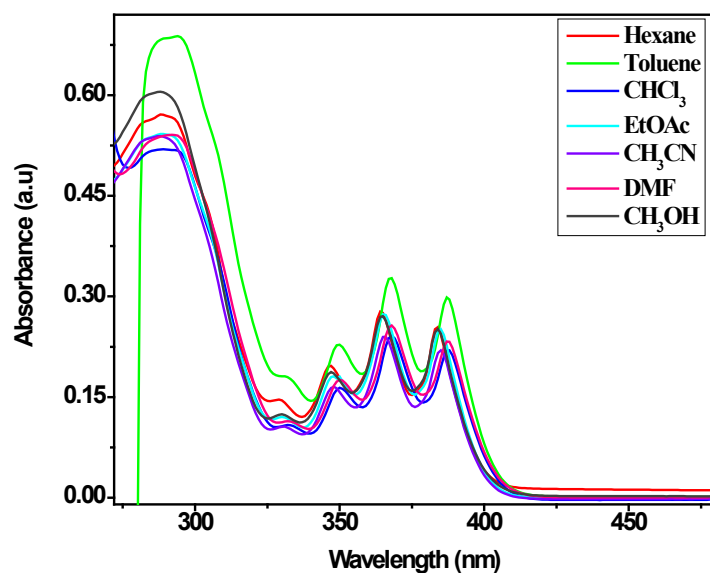


Fig. 11 UV-Vis absorption spectra of **4a** in different solvents (1×10^{-5} M) carried out at ambient temperature.

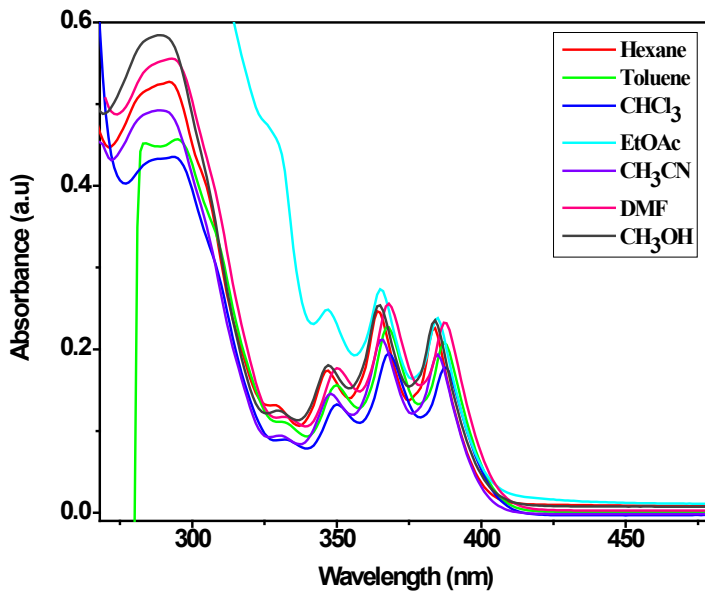


Fig. 12 UV-Vis absorption spectra of **4b** in different solvents (1×10^{-5} M) carried out at ambient temperature.

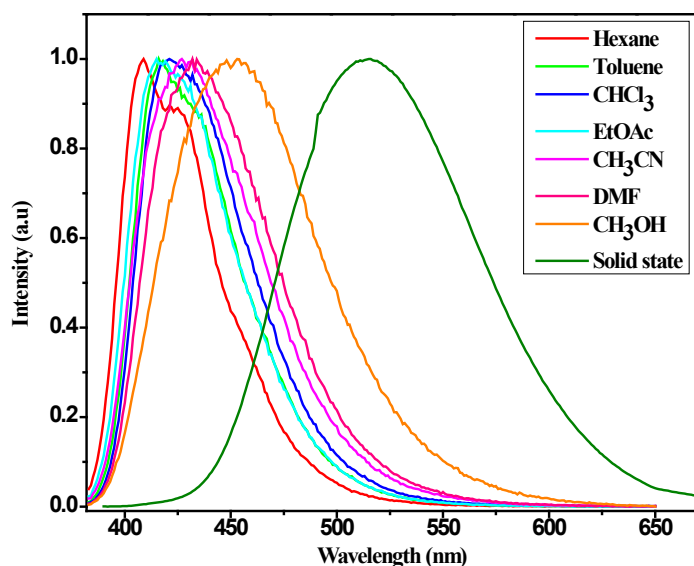


Fig. 13 Normalized emission spectra of **4b** in different solvents (1×10^{-5} M) and in solid state carried out at ambient temperature.

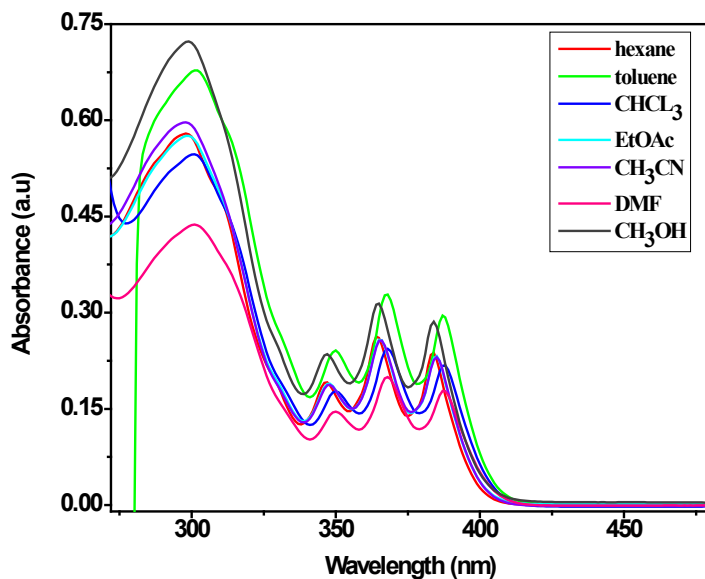


Fig. 14 UV-Vis absorption spectra of **4c** in different solvents (1×10^{-5} M) carried out at ambient temperature.

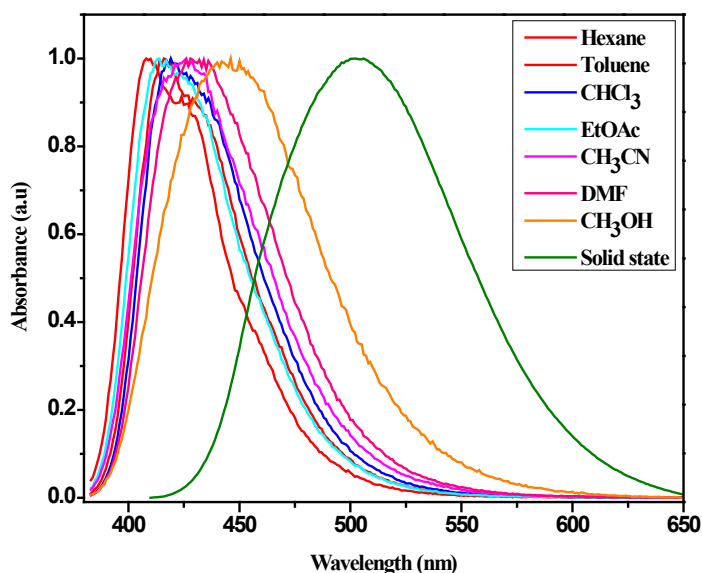


Fig. 15 Normalized emission spectra of **4c** in different solvents (1×10^{-5} M) and in solid state carried out at ambient temperature.

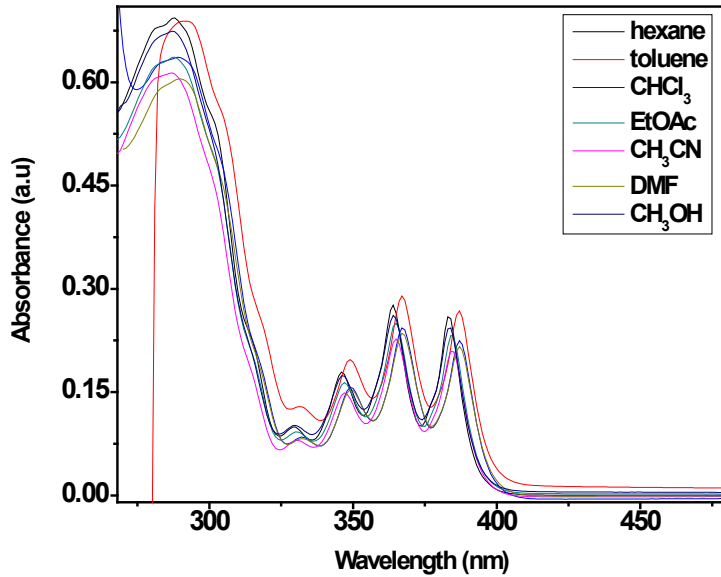


Fig. 16 UV-Vis absorption spectra of **8a** in different solvents (1×10^{-5} M) carried out at ambient temperature.

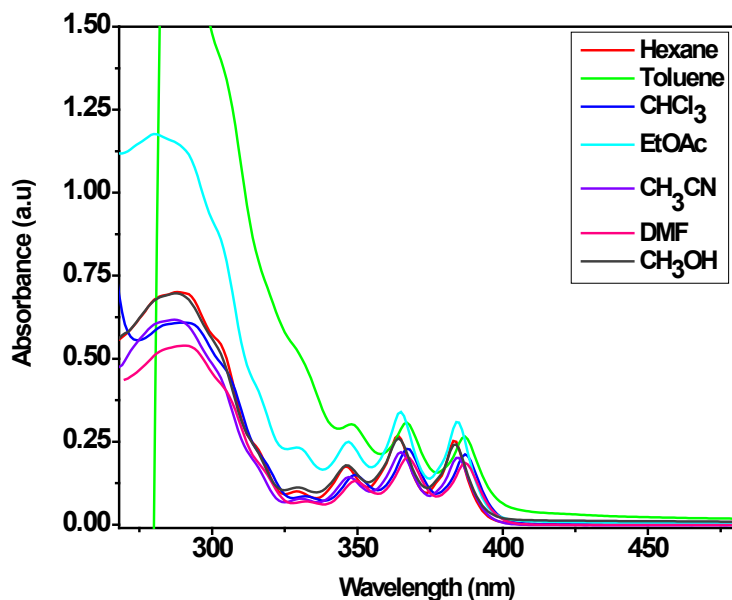


Fig. 17 UV-Vis absorption spectra of **8b** in different solvents (1×10^{-5} M) carried out at ambient temperature.

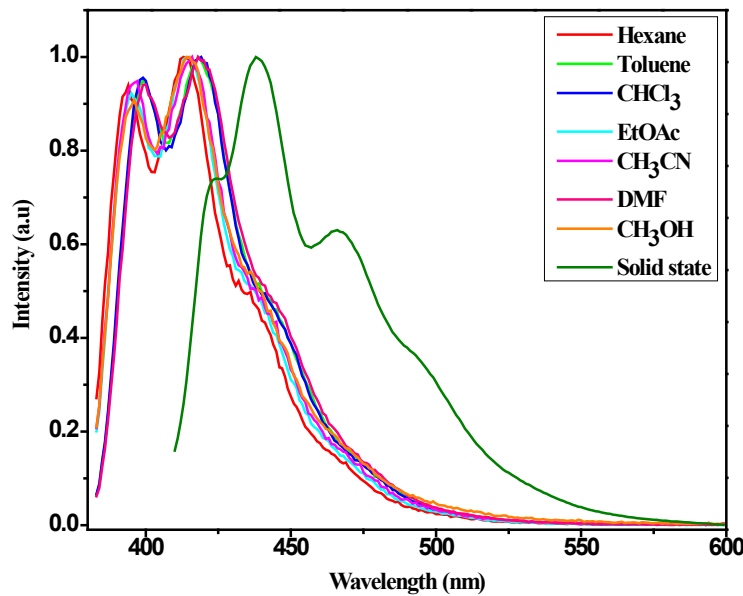


Fig. 18 Normalized emission spectra of **8b** in different solvents (1×10^{-5} M) and in solid state carried out at ambient temperature.

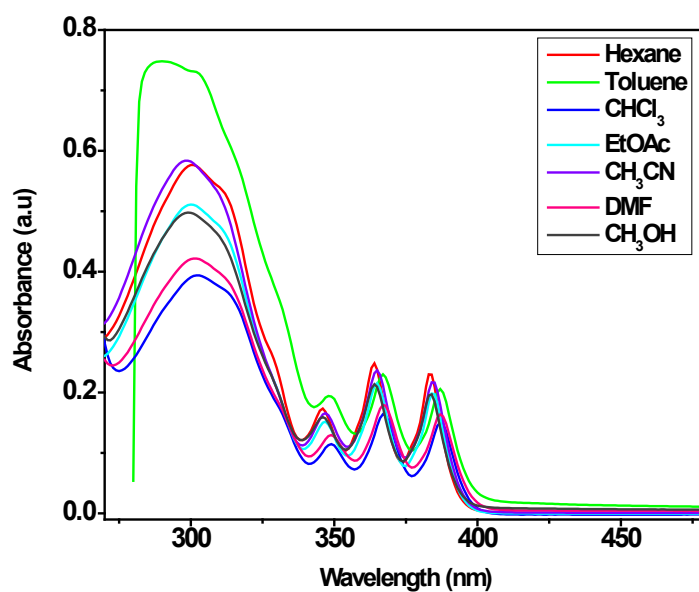


Fig. 19 UV-Vis absorption spectra of **8c** in different solvents (1×10^{-5} M) carried out at ambient temperature.

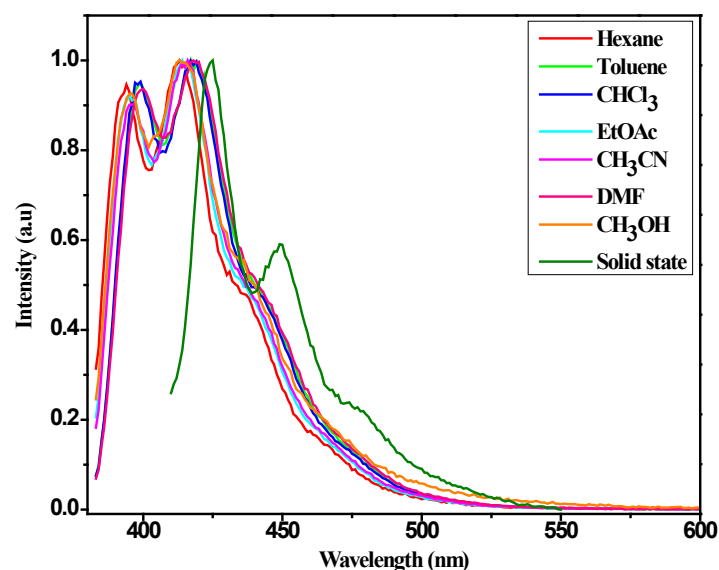
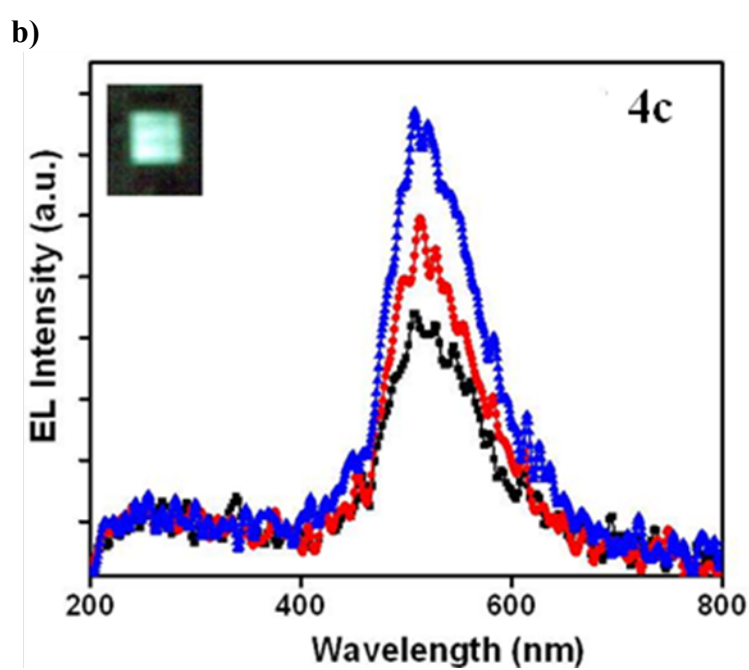
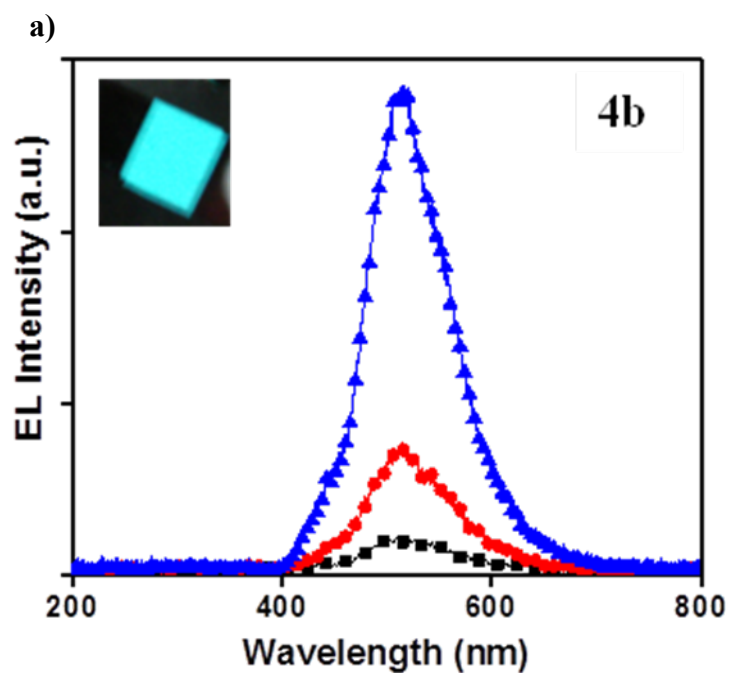


Fig. 20 Normalized emission spectra of **8c** in different solvents (1×10^{-5} M) and in solid state carried out at ambient temperature.



c)

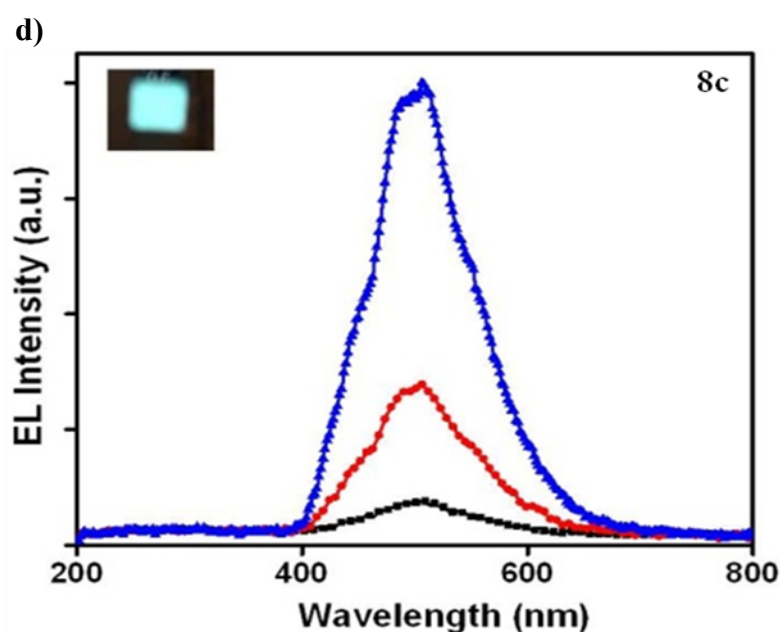
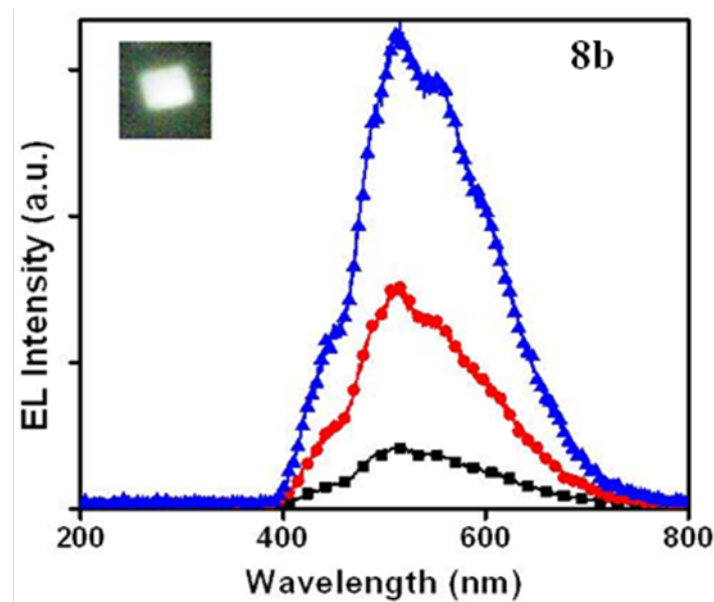
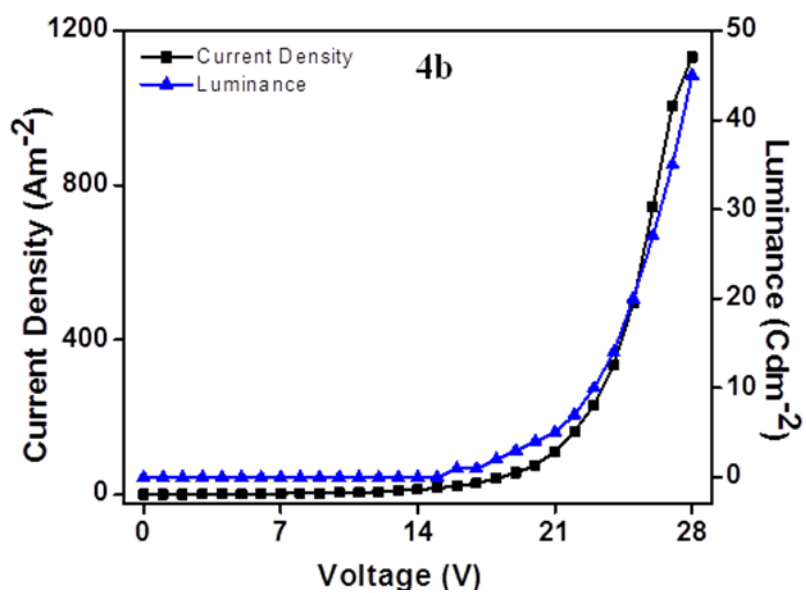
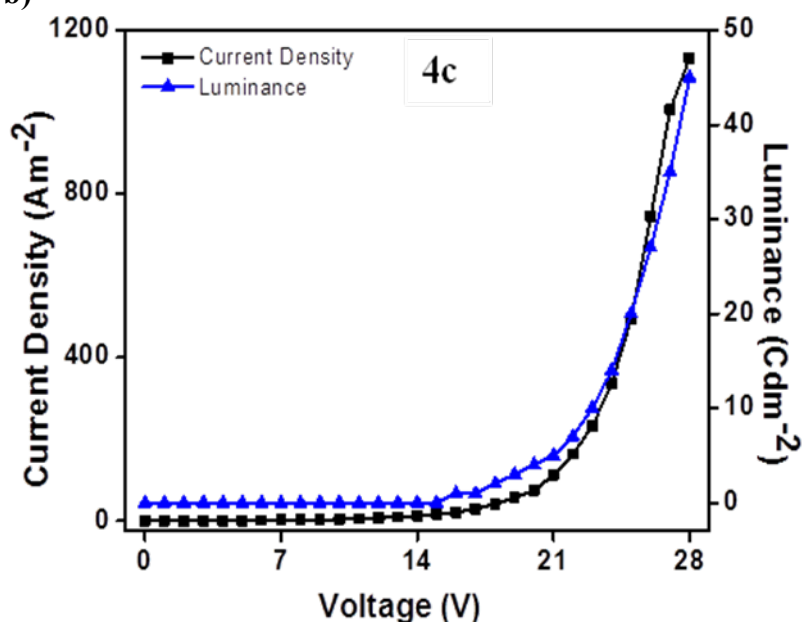


Fig. 21 The characteristic EL performance data for **4b** (a), **4c** (b), **8b** (c) and **8c** (d) at 10, 12, 14V.

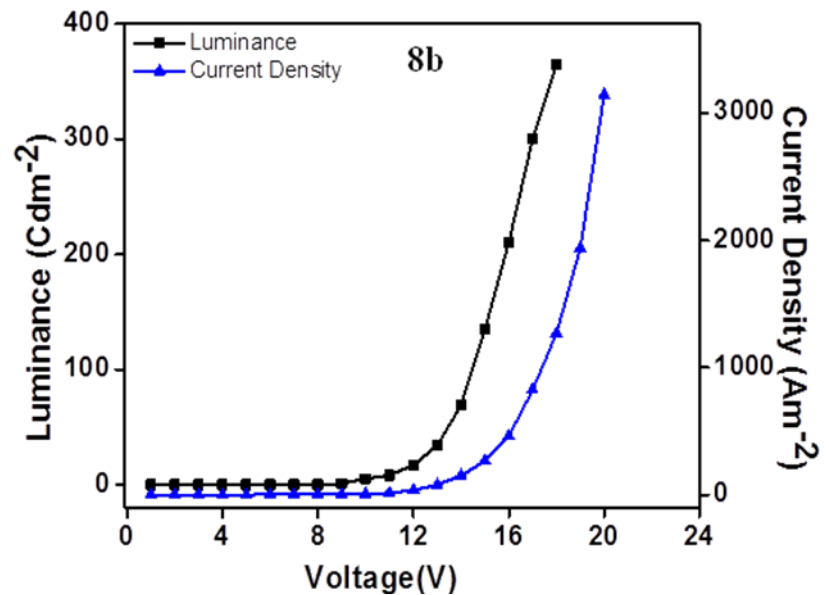
a)



b)



c)



d)

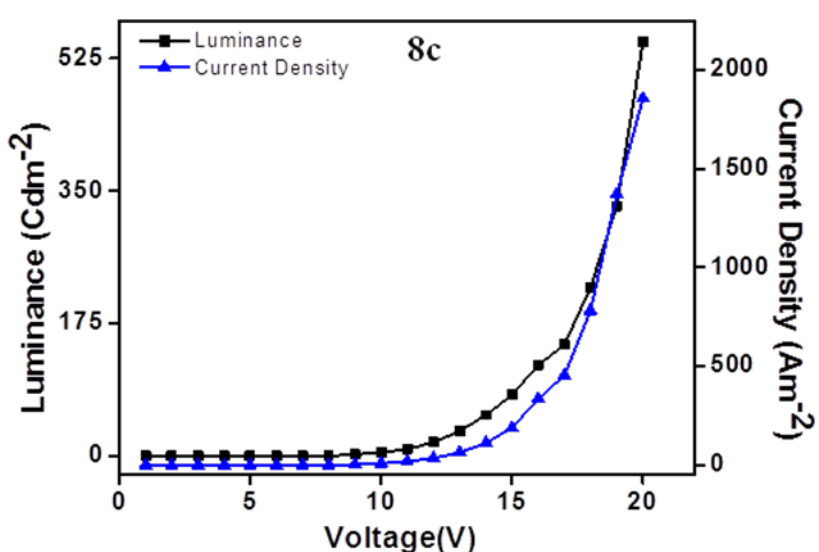
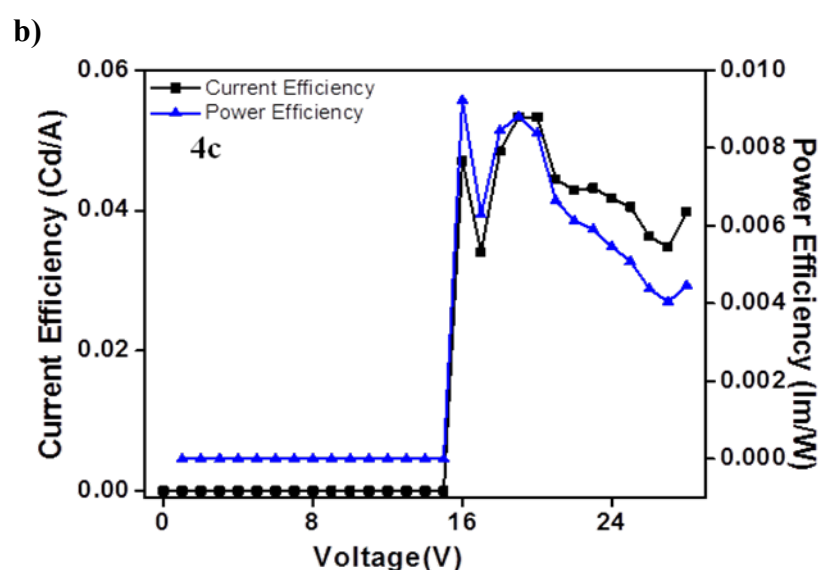
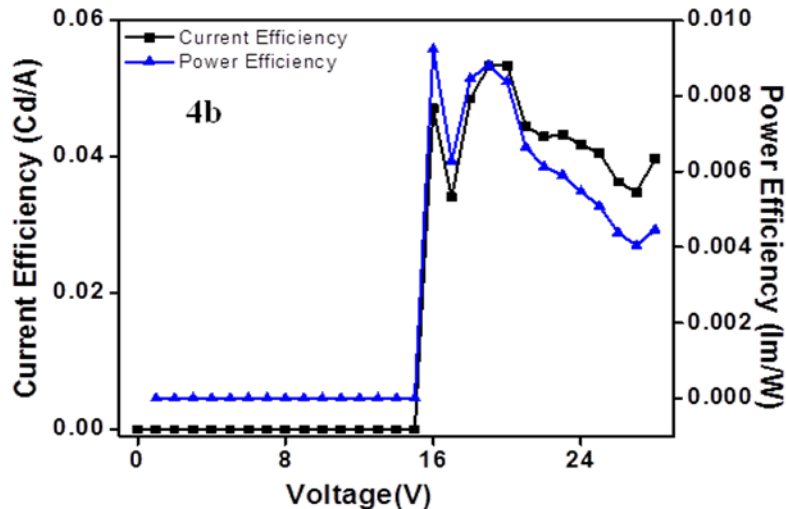
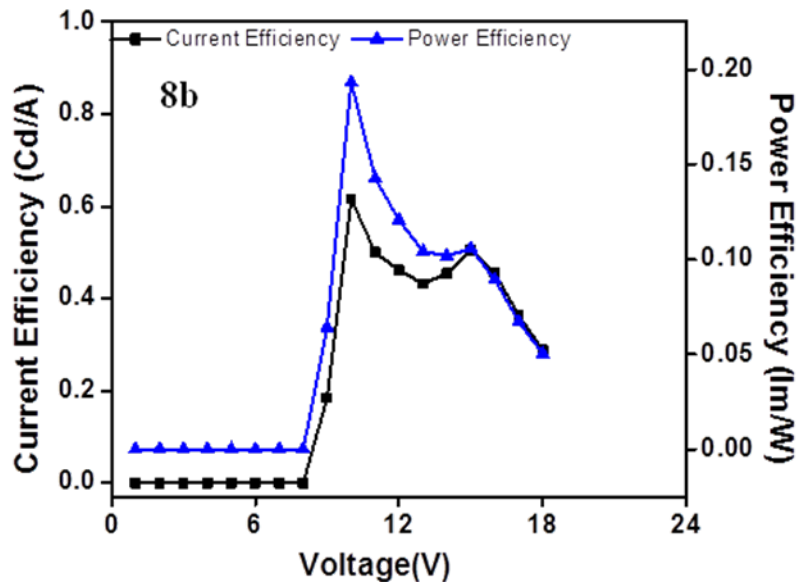


Fig. 22 Current density and luminance curve for **4b** (a), **4c** (b), **8b** (c) and **8c** (d)

a)



c)



d)

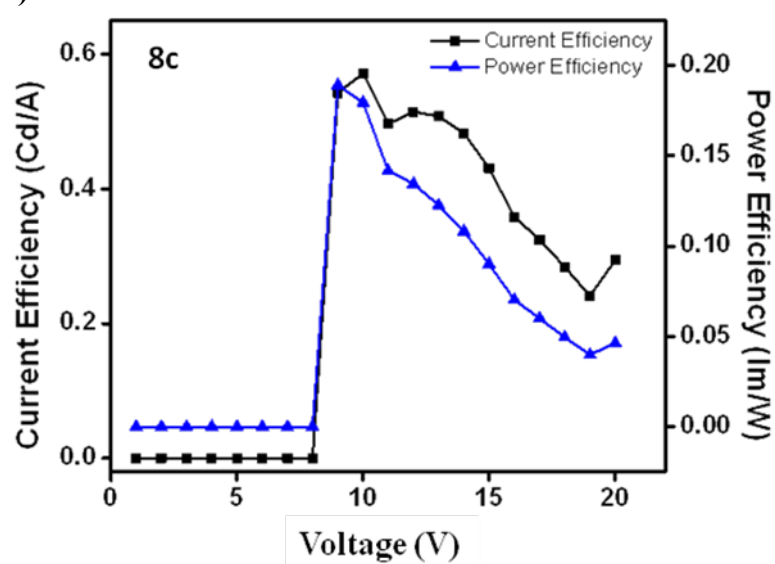


Fig. 23 Current and power efficiency curve for **4b** (a), **4c** (b), **8b** (c) and **8c** (d)

Table 1. Crystal data and structure refinement details for **4b** and **8c**.

	4b	8c
Empirical formula	C ₃₂ H ₂₆ N ₂ O	C ₃₁ H ₂₄ N ₂ O ₄
Formula weight	454.55	488.52
Temperature	294(2) K	294(2) K
Wavelength	0.71073 Å	0.71073 Å
Crystal system	Monoclinic	Monoclinic
Space group	<i>P2</i> <i>1/c</i>	<i>P2</i> <i>1/c</i>
Unit cell dimensions	<i>a</i> = 20.2645(11) Å α = 90°. <i>b</i> = 12.2263(6) Å β = 94.5970(10)° <i>c</i> = 10.0739(5) Å γ = 90°.	<i>a</i> = 19.3466(14) Å α = 90° <i>b</i> = 16.8505(12) Å β = 100.6960(10)° <i>c</i> = 7.7163(6) Å, γ = 90°
Volume	2487.9(2) Å ³	2471.8(3) Å ³
Z	4	4
Density (calculated)	1.214 Mg m ⁻³	1.313 Mg m ⁻³
Absorption coefficient	0.073 mm ⁻¹	0.087 mm ⁻¹
F(000)	960	1024
Crystal size	0.21 x 0.12 x 0.11 mm ³	0.19 x 0.17 x 0.09 mm ³
θ range for data collection	1.01 to 25.00°.	1.61 to 25.00°.
Index ranges	-24 ≤ <i>h</i> ≤ 24, -14 ≤ <i>k</i> ≤ 14, -11 ≤ <i>l</i> ≤ 11	-22 ≤ <i>h</i> ≤ 22, -20 ≤ <i>k</i> ≤ 20, -9 ≤ <i>l</i> ≤ 9
Reflections collected	23497	23465
Independent reflections	4370 [<i>R</i> _{int} = 0.0329]	4338 [<i>R</i> _{int} = 0.0301]
Completeness to θ = 25.00°	100.0 %	100.0 %
Refinement method	Full-matrix least-squares on <i>F</i> ₂	Full-matrix least-squares on <i>F</i> ₂
Data / restraints / parameters	4370 / 0 / 319	4338 / 0 / 337
Goodness-of-fit on F2	1.059	1.226
Final R indices [I > 2 σ(I)]	<i>R</i> 1 = 0.0602, <i>wR</i> 2 = 0.1613	<i>R</i> 1 = 0.0580, <i>wR</i> 2 = 0.1236

R indices (all data)	$RI = 0.0792, wR2 = 0.1795$	$RI = 0.0660, wR2 = 0.1277$
Largest diff. peak and hole	$0.374 \text{ and } -0.139 \text{ e.}\AA\text{-}3$	$0.184 \text{ and } -0.147 \text{ e.}\AA\text{-}3$

Table 2. UV-Vis absorption data (λ_{abs}) of **4a–4c** and **8a–8c** in different solvents.

Compound ^a	Toluene (nm) (ϵ) ^b	EtOAc (nm) (ϵ) ^b	CH ₃ CN (nm) (ϵ) ^b	DMF (nm) (ϵ) ^b
4a	294(68800), 350(22800), 3683(2700), 387(29900)	288(54000), 348(18100), 365(27300), 385(25100)	288(53900), 348(16500), 366(24000), 385(21900)	292(54100), 350(17600), 368(25600), 387(23300)
4b	295(45700), 350(15600), 368(22700), 387(20800)	292(18900), 347(24800), 365(27400), 385(23800)	289(49200), 348(14500), 366(21100), 385(19300)	293(55500), 350(17700), 368(25500), 387(23200)
4c	302(64600), 350(24100), 368(32800), 387(29600)	299(57600), 348(18900), 365(25800), 385(23200)	298(59700), 348(18800), 366(25600), 385(23100)	301(43700), 350(14500), 368(12000), 387(17800)
8a	292(68900), 349(19700), 367(28900), 387(26800)	288(63700), 347(16400), 365(25000), 384(23200)	287(61300), 347(14900), 365(22700), 384(20900)	290(60500), 349(15300), 367(23500), 387(21600)
8b	285(194500), 348(30300), 367(30700), 387(26500)	280(17600), 347(25000), 365(34000), 384(30900)	287(61700), 347(14400), 365(21900), 384(20100)	290(53900), 349(13100), 367(20200), 387(18600)
8c	303(73200), 348(19500), 367(23000), 387(20600)	300(50900), 347(15200), 365(21500), 384(19800)	299(58400), 347(16600), 365(23700), 384(21700)	301(42200), 349(13000), 367(18000), 387(16400)

^a All the compounds measured in 1×10^{-5} M concentration, at room temperature,

^b Molar extinction coefficient (ϵ , mol⁻¹ cm⁻¹).

¹H and ¹³C-NMR spectra for **4a-4c** and **8a-8c**.

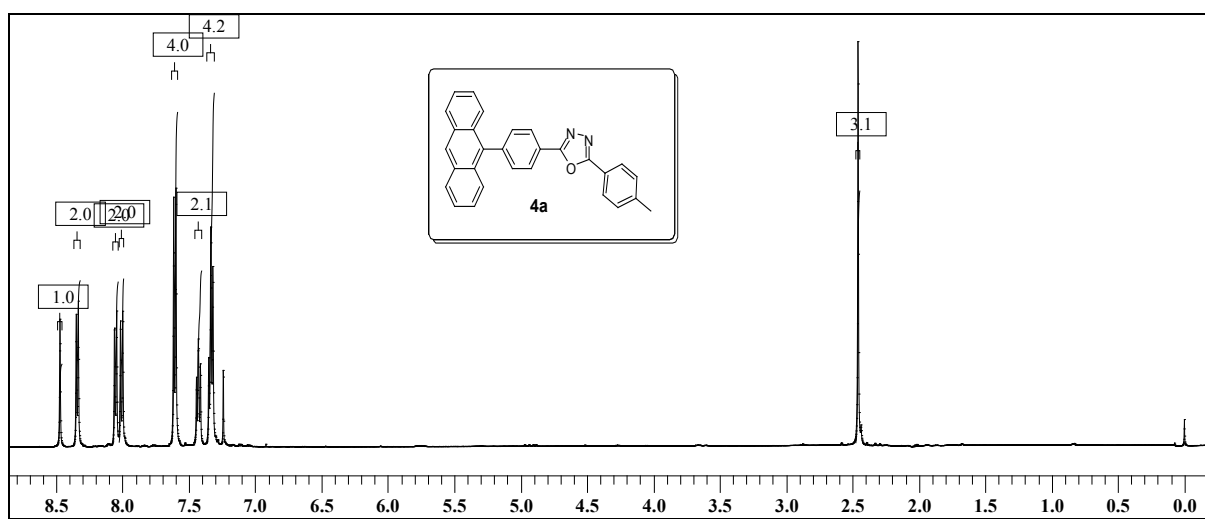


Fig. 24 ¹H NMR spectrum of compound **4a**

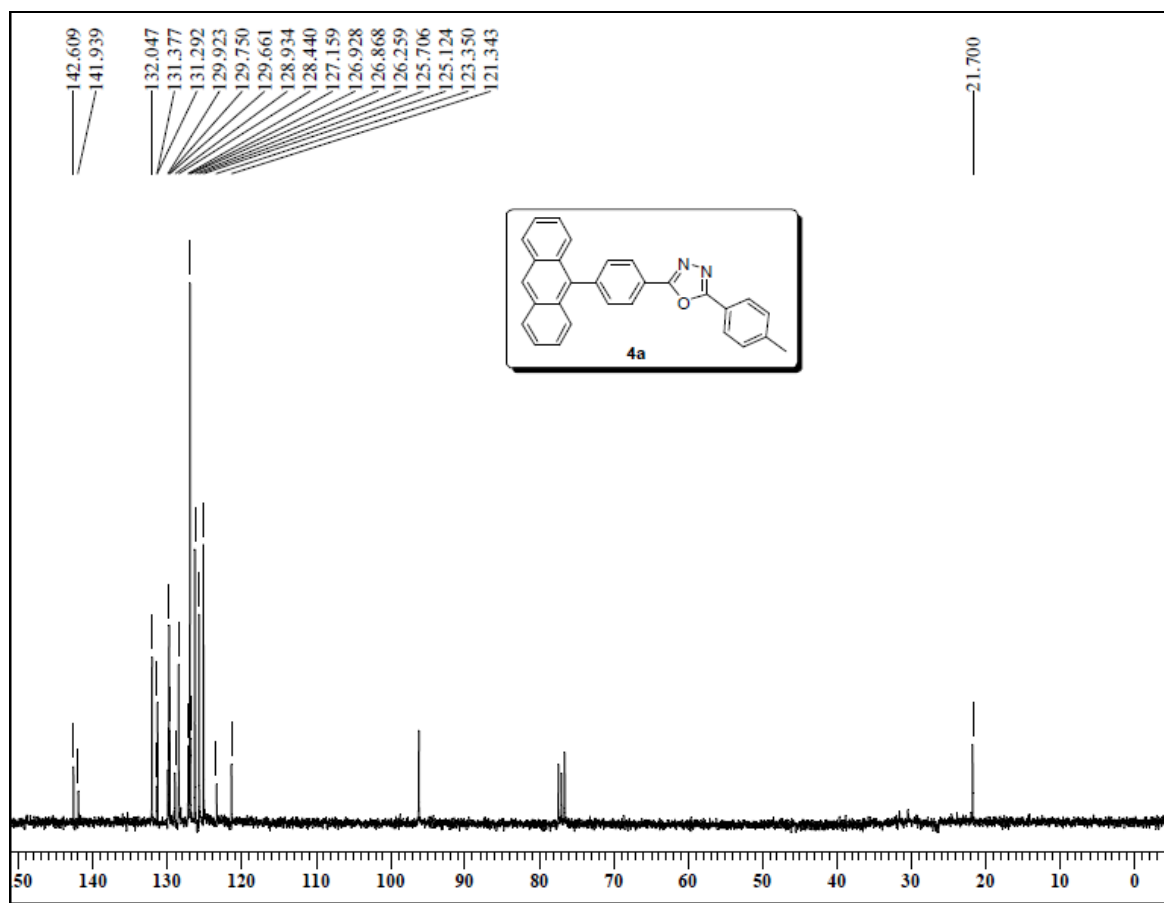


Fig. 25 ¹³C NMR spectrum of compound **4a**

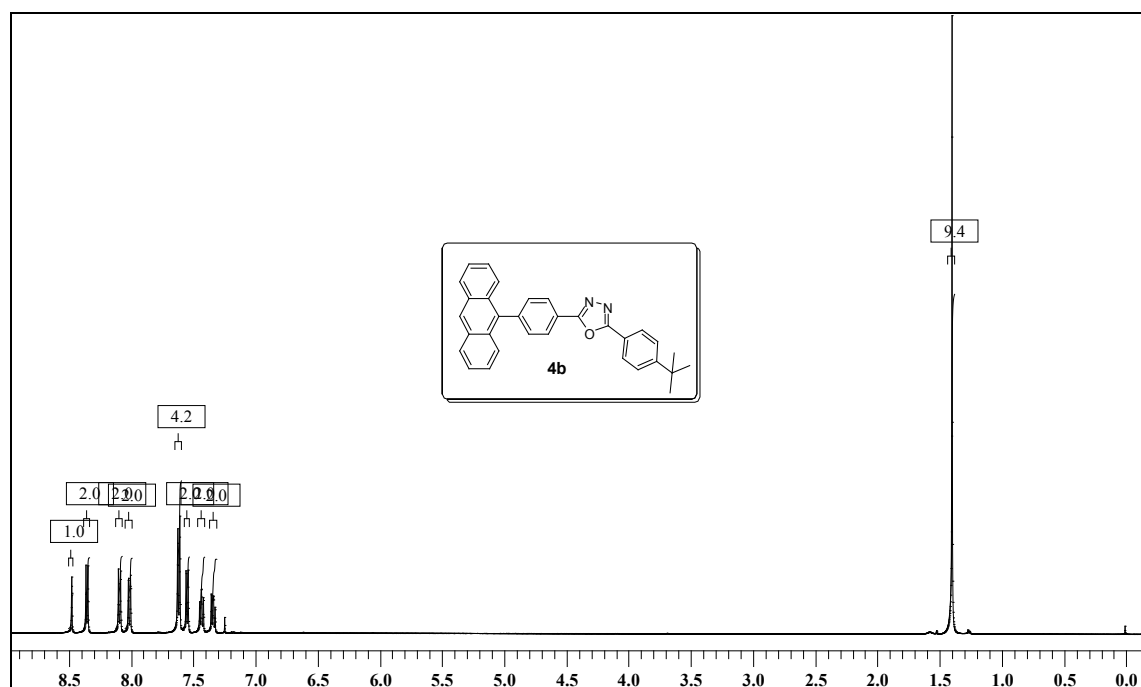


Fig. 26 ¹H NMR spectrum of compound 4b

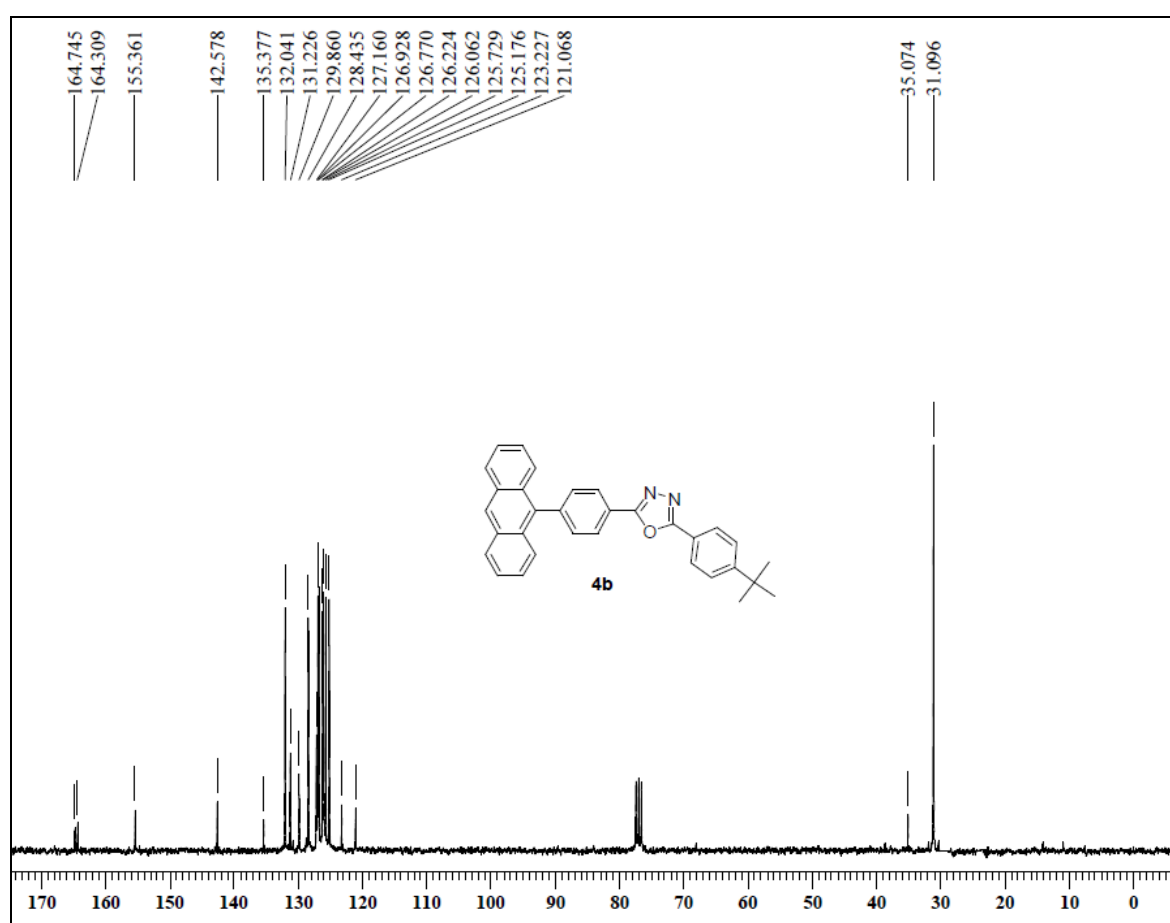


Fig. 27 ¹³C NMR spectrum of compound 4b

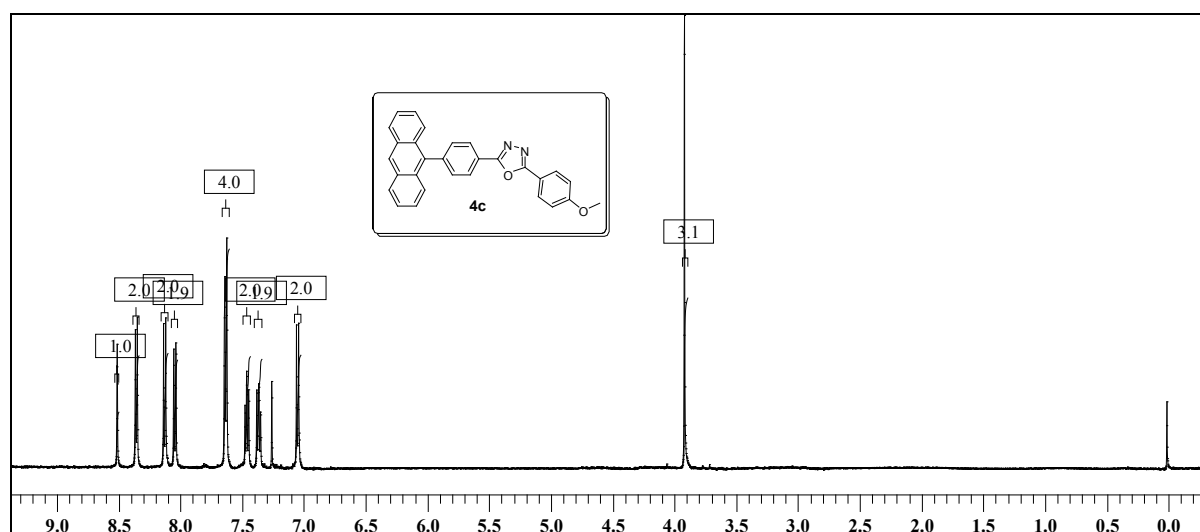


Fig. 28 ¹H NMR spectrum of compound 4c

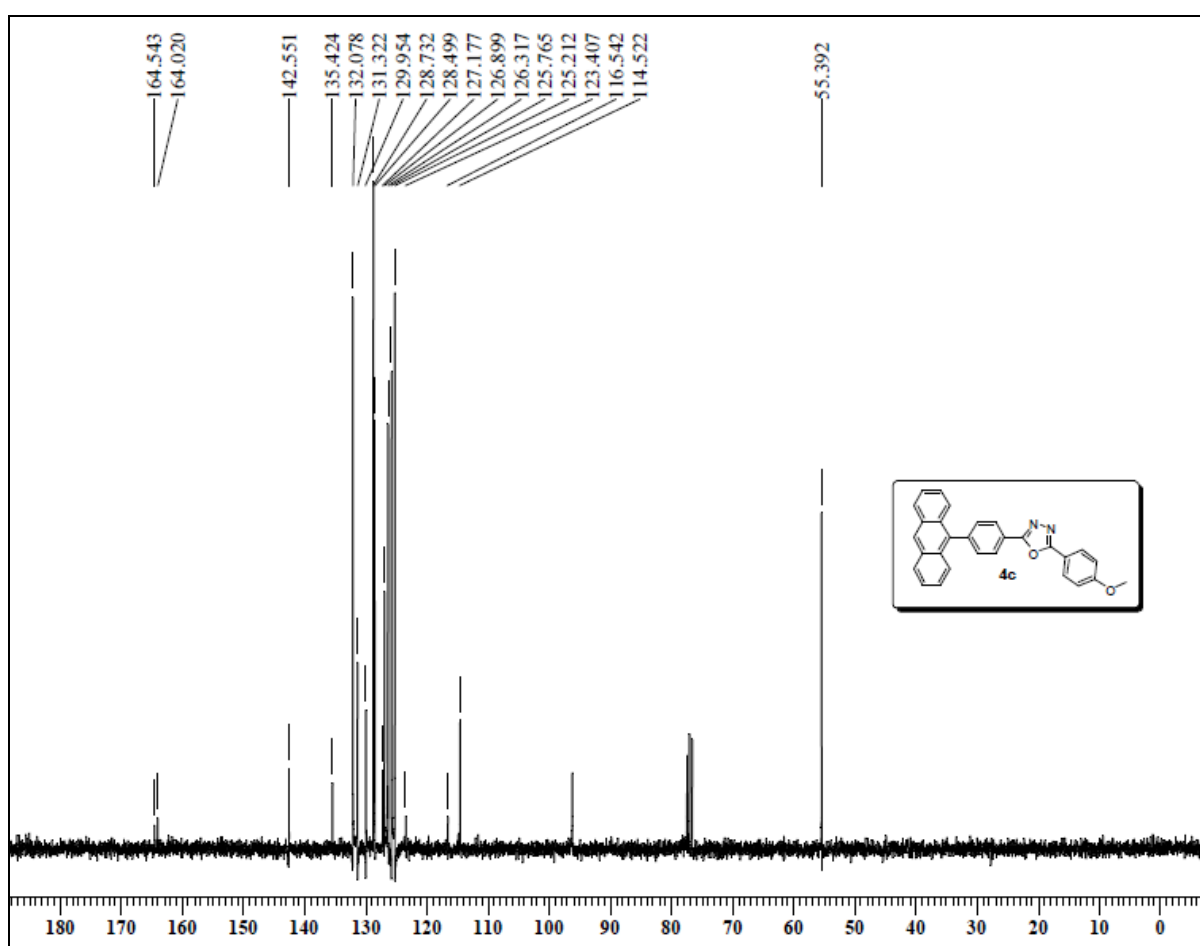


Fig. 29 ¹³C NMR spectrum of compound 4c

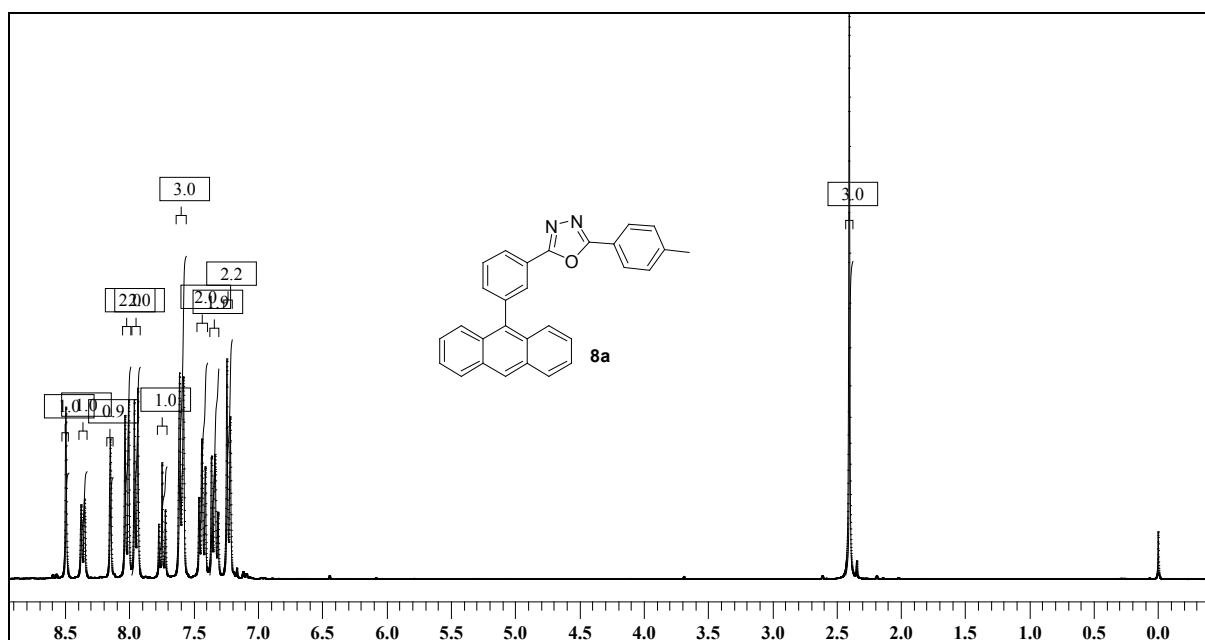


Fig. 30 ¹H NMR spectrum of compound 8a

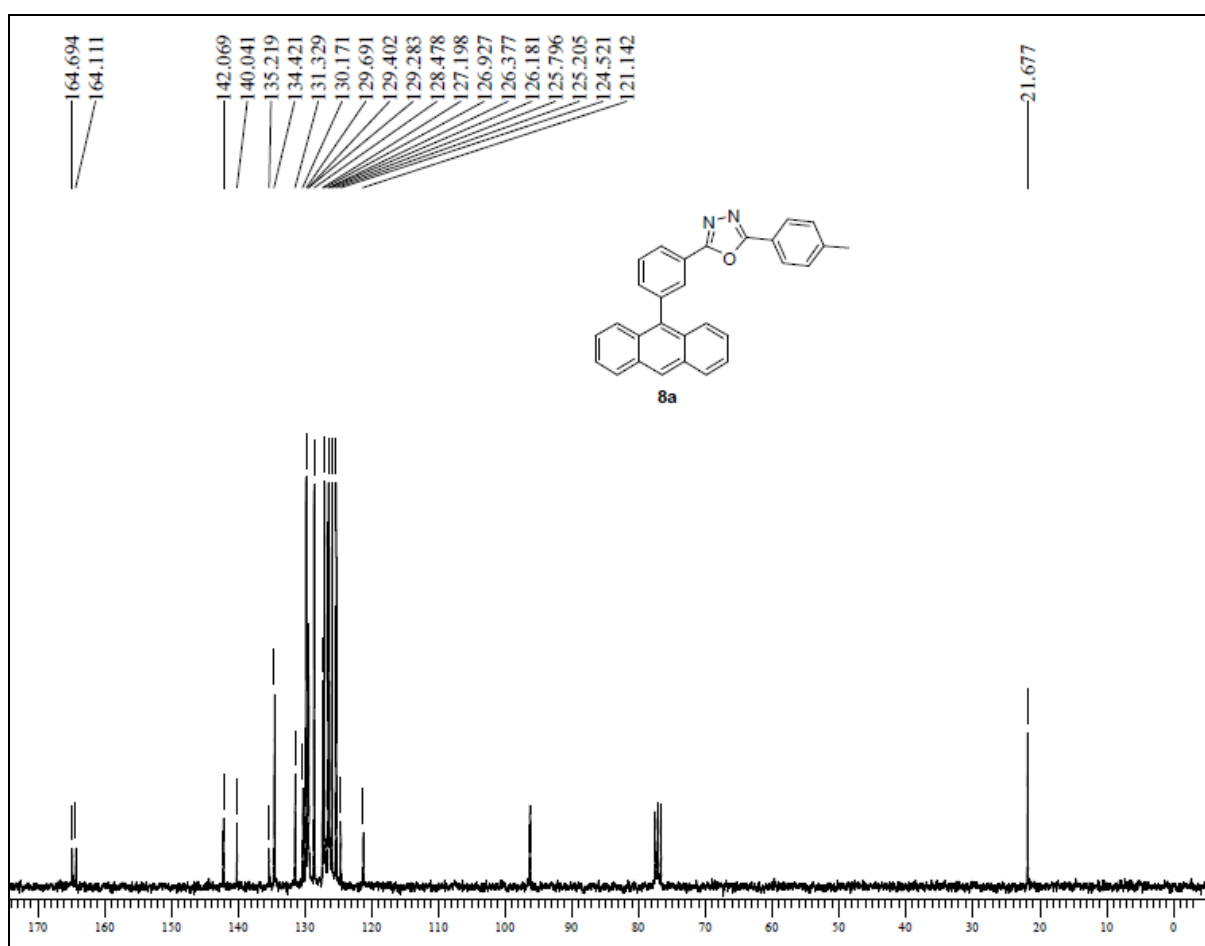


Fig. 31 ¹³C NMR spectrum of compound 8a

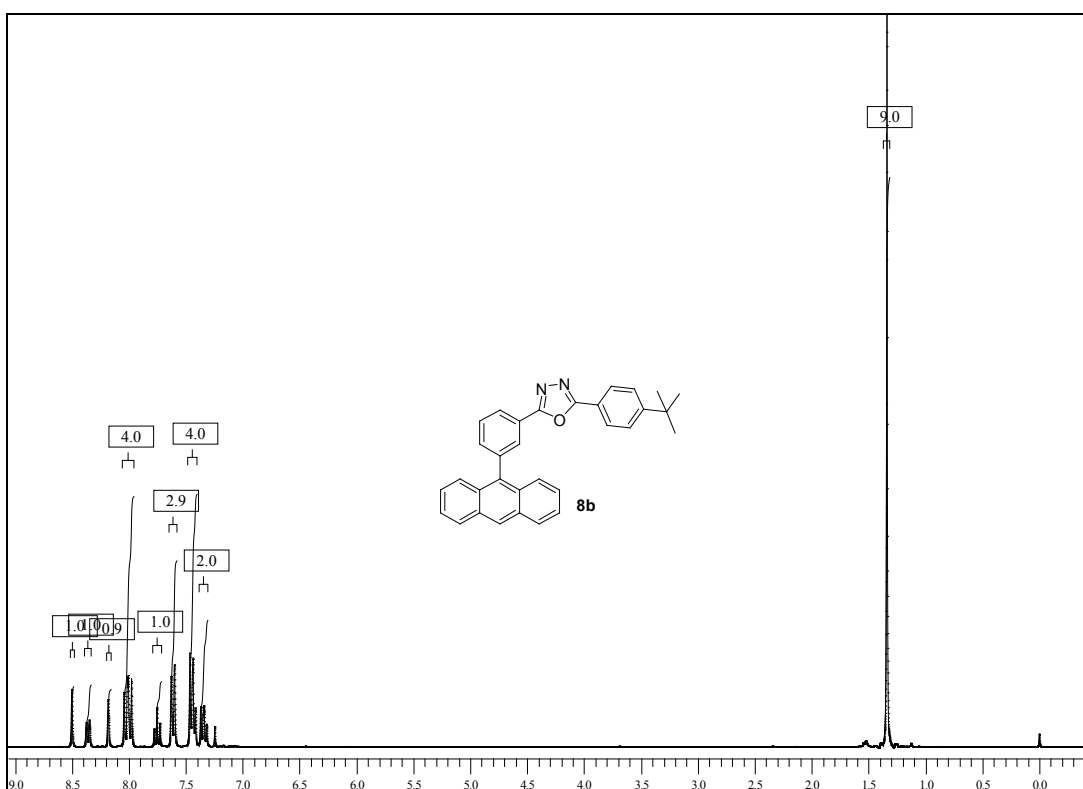


Fig. 32 ¹H NMR spectrum of compound 8b

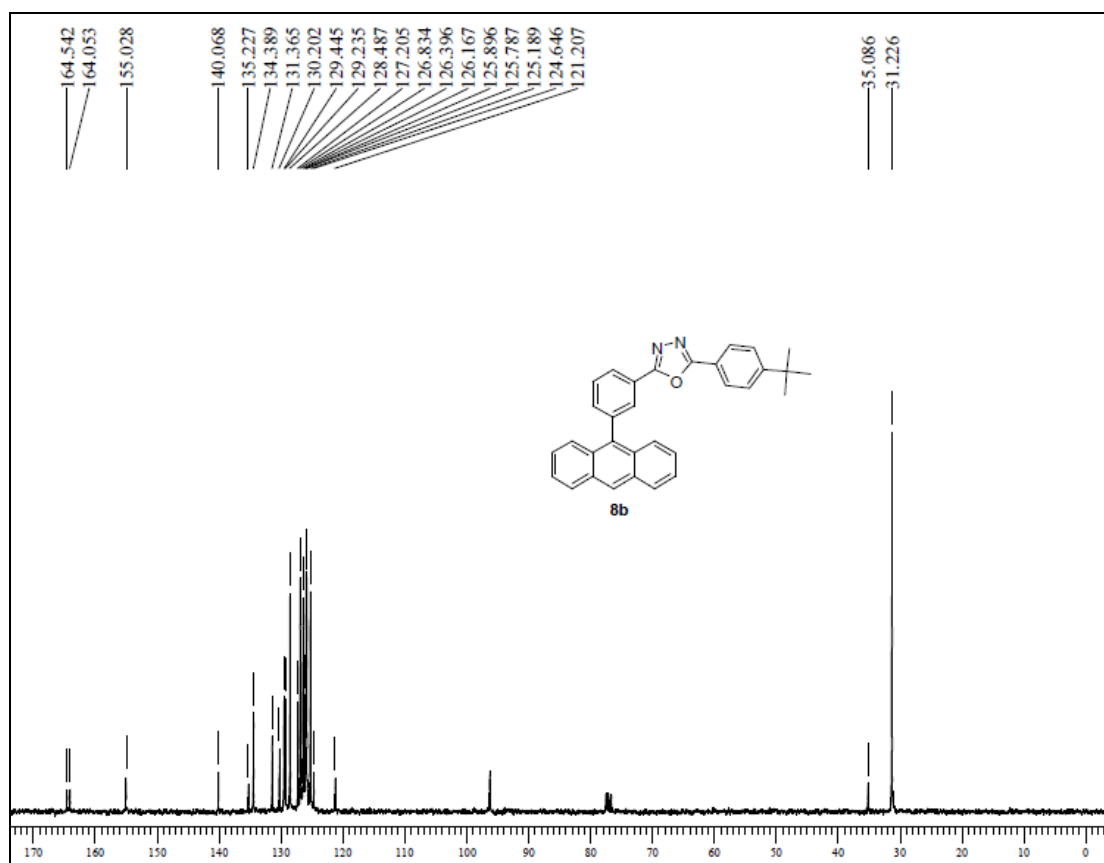


Fig. 33 ¹³C NMR spectrum of compound 8b

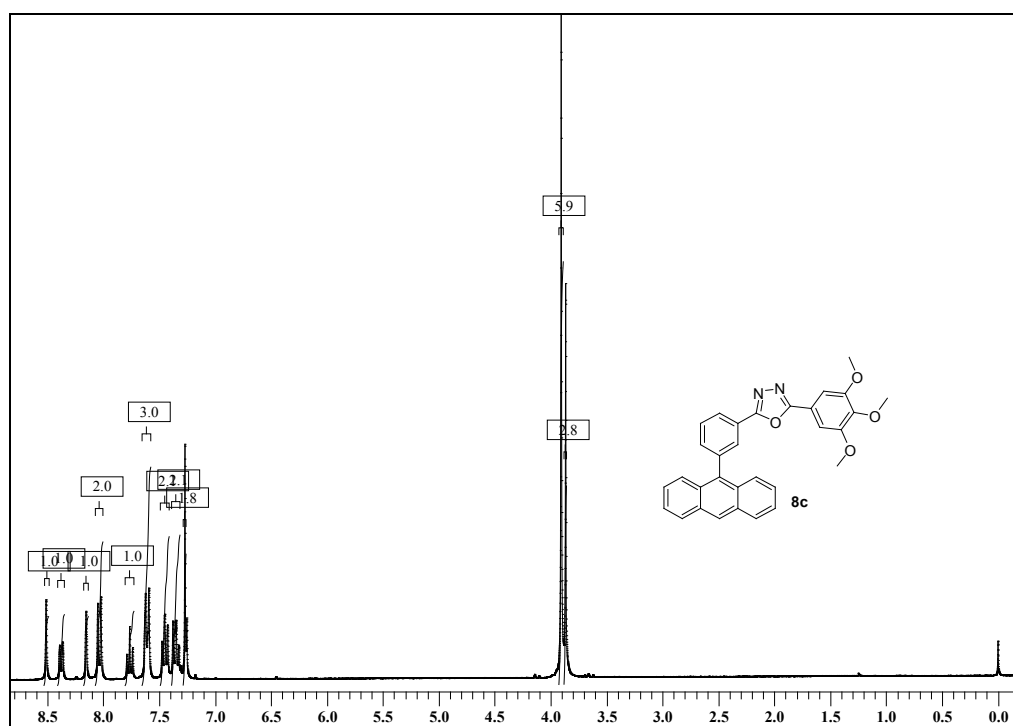


Fig. 34 ¹H NMR spectrum of compound 8c

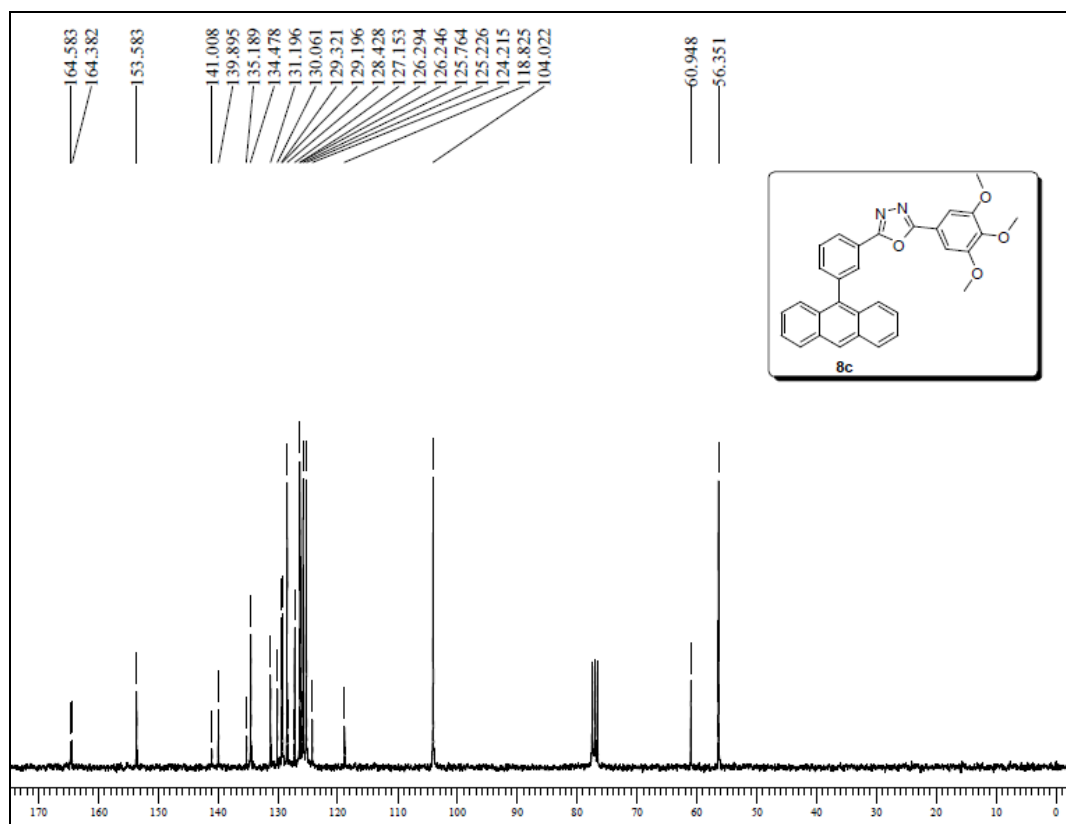


Fig. 35 ¹³C NMR spectrum of compound 8c